ELSEVIER

Journal of Power Sources 109 (2002) 189–202

JOURNAL OF POWER SOURCES

www.elsevier.com/locate/jpowsour

Failure mechanisms in valve regulated lead/acid batteries for cyclic applications

R.J. Ball[a,*], R. Kurian[b], R. Evans[c], R. Stevens[a]

[a]*Department of Engineering and Applied Science, University of Bath, Bath BA2 7AY, UK*
[b]*Hawker Ltd., Stephenson St., Newport NP9 OXJ, UK*
[c]*Invensys, Westinghouse site, Chippenham, Wiltshire SN15 1SJ, UK*

Received 9 September 2001; received in revised form 17 January 2002; accepted 22 January 2002

Abstract

Valve regulated lead/acid (VRLA) batteries are used in a variety of different applications, one of which is cycling. Cycle life testing of a batch of 40 Ah VRLA batteries showed a large variation in the cycles to failure ranging from 10 to 133 cycles. Further testing and the destructive examination of these batteries provided information on the likely causes of failure. Results from monitoring reduction in cell voltage during a final discharge/charge cycle, scanning electron microscopy (SEM), BET surface area analysis, X-ray diffraction, interfacial analysis and electron probe analysis, were used to identify the failure mechanisms occurring within the batch. Batteries that failed after a low number of cycles, 10 and 28, were believed to have done so due to sulphation of the positive plate. Thick corrosion layers were shown to be the cause of failure in the batteries that sustained high numbers of cycles, 92 and 133. Results suggested that batteries failing at intermediate numbers of cycles, 42, 49, 65 and 73, failed due to degradation of the cells simultaneously and a single failure mechanism could not be identified.

Keywords: VRLA; Cycle life; Positive electrode

1. Introduction

A significant proportion of the valve regulated lead/acid (VRLA) batteries currently produced are for use in cyclic applications. An understanding of the compositional and structural changes that occur within a battery during repeated cycling is important if failure mechanisms are understood and battery designs to be improved.

Cycling data obtained from a single batch of 40 Ah VRLA batteries, indicated that they were failing after different numbers of cycles. These batteries were manufactured using the same starting material and processing technique, so were expected to show similar cycle lives. Differences in cycle life can only be explained by the inherent variability of the materials and processes that occur within each batch of batteries during manufacture, that are not detectable from the usual quality control procedures. Care was taken in the production of the cells and batteries to ensure standard procedures, thereby producing a product as uniform as possible. Details of the production process are of necessity confidential. In this paper, results obtained from the examination of a number of batteries from the same batch that failed after different numbers of cycles is discussed.

2. Production of test batteries

The batteries examined in this study were all 40 Ah, 12 V monobloc units of the same design and constructed using identical materials. Positive electrodes were produced using a standard grey oxide positive paste. The negative paste mix was also manufactured from grey oxide. Positive and negative grids were produced from a proprietary lead alloy. Glass microfibre separators were used, consisting of 70% coarse and 30% fine fibres. Assembled batteries were filled with electrolyte of specific gravity (SG) 1.290 at 15.5 °C prior to formation.

3. Cycling of test batteries

Cycling was carried out automatically using Digitron charging units. Each cycle consisted of a constant current discharge at 7.05 A to 10.2 V followed by a constant voltage

* Corresponding author. Tel.: +44-1225-826826; fax: +44-1225-826098.
E-mail address: r.j.ball@bath.ac.uk (R.J. Ball).

0378-7753/02/$ – see front matter
PII: S0378-7753(02)00071-X

recharge at 14.7 V for 16 h. This was repeated until the capacity after charging was less than 80% of the starting capacity.

4. Experimental methods

4.1. Characterisation of cells

The reduction in capacity of all cycled batteries can be attributed to changes that have occurred in the individual cells. However, the extent to which these destructive processes have developed in each cell is often different. Any variations can be quantified by measuring the reduction in voltage of each cell with time.

A series 1200 GRANT Squirrel data logger, was used to log individual cell voltages with time. Connections from each cell to the data logger were made by inserting nails through the battery case lid into the underlying cast-on straps. Each cell was connected to a different channel of the data logger prior to the battery being subjected to a C1 (100% depth of discharge in 1 h) capacity discharge to 6 V. The discharge current was 27.6 A and recharge voltage 14.7 V. Voltages were logged at 1 min intervals. After discharge, the battery was recharged and squirrel data downloaded into a PC and displayed on an Excel spreadsheet. Connections made between the cells of the battery and data logger are shown diagrammatically in Fig. 1. The cells which had the greatest and least reduction in voltage were removed for examination and referred to as the bad and good cells, respectively.

4.2. Destructive examination of test batteries

All batteries were destructively examined, in the charged state, to allow detailed analysis of individual electrodes. In order to remove the battery cells for examination, it was necessary to gain access to the interior of the battery. This was done by firstly removing the polypropylene battery lid as shown in Fig. 2. The good and bad cells were then removed from the battery case for further examination by cutting the connecting weld and pulling the cell directly upwards, out of the battery case.

Once the cells had been removed from the battery case, the positive electrodes were separated for examination. This was achieved by pulling off the cast-on straps with a pair of pliers, which conveniently doubled as an integrity check for the welds between the electrode and cast-on strap. A cell with one cast-on-strap partly removed is shown in Fig. 3.

Measurements of the SG of the electrolyte were taken, using a surface tension method, at the top and bottom of each cell, to allow the extent of acid stratification to be assessed. Electrolyte was obtained by squeezing it out from a sample of the separator paper taken from a representative position within the cell.

Representative positive plates, from both good and bad cells, were placed in a beaker of distilled water for approximately 30 min to dilute and remove acid. Plates were rinsed with industrial methylated spirits and placed in a vacuum oven at 60 °C for 24 h or until totally dried. After the plates had dried, the oven heater was switched off and the plates were allowed to cool down to room temperature whilst still under vacuum to prevent oxidation. Dried plates were then

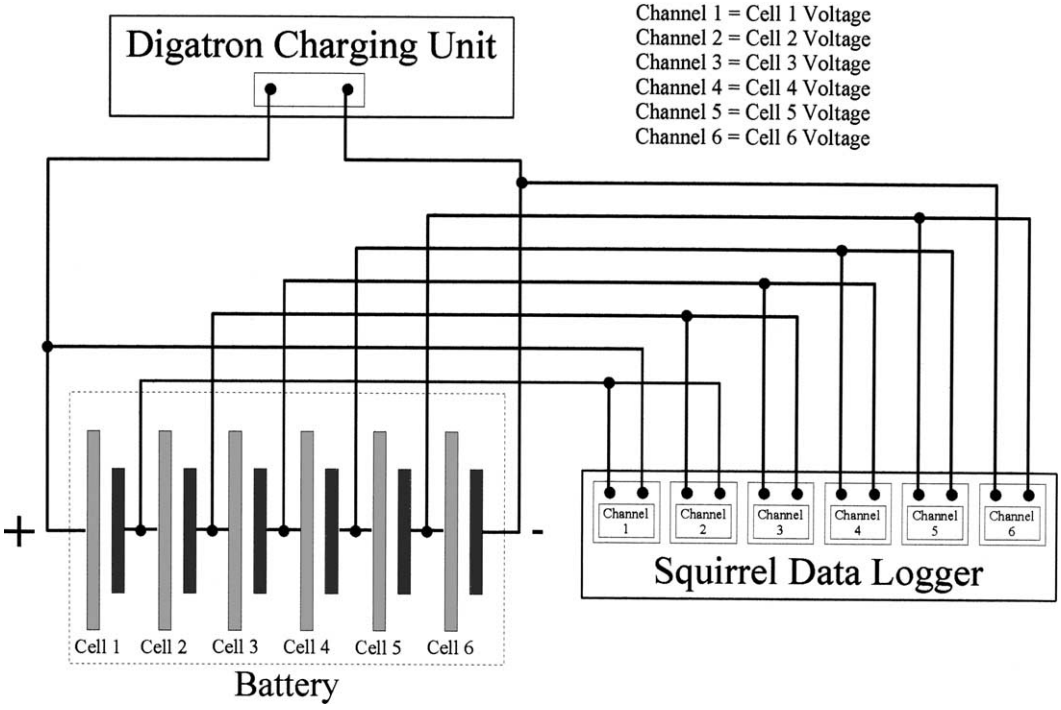

Fig. 1. Circuit used to monitor voltages of individual cells during a discharge/charge cycle.

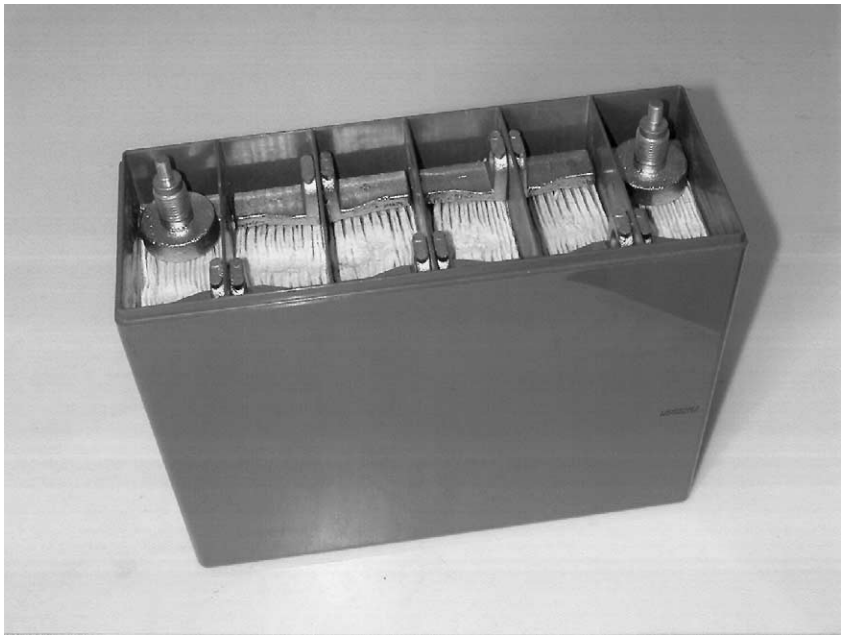

Fig. 2. A 12 V six cell monobloc with lid removed.

stored in a dessicator, containing silica gel, before further examination and analysis. It should be noted that despite the care taken to preserve the plates lead oxide is prone to self decomposition, whereby oxygen is evolved [1]. For this reason, results indicating oxide stoichiometry of the corrosion layer should be viewed as being pessimistic in terms of oxygen concentration. Negative plates were not examined, as the high surface area sponge lead of which they consist is highly reactive and it was practically impossible to remove the plates without the formation of oxide on their surface.

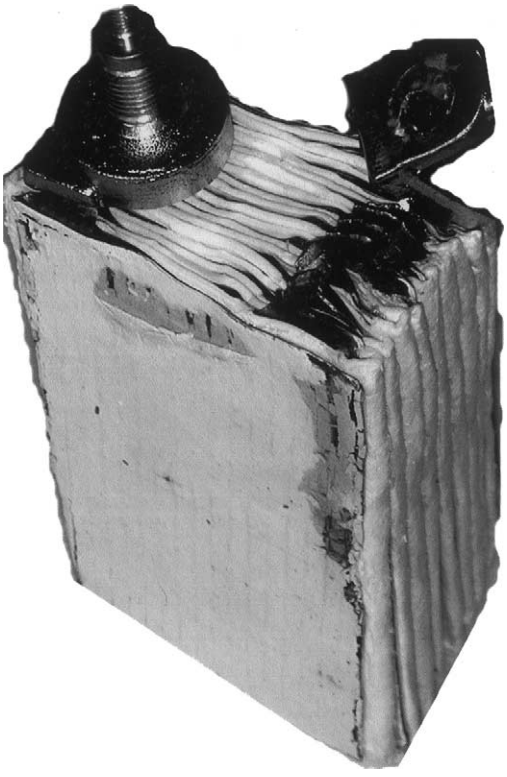

Fig. 3. Cell removed from battery showing cast-on strap partly removed.

4.3. Scanning electron microscopy (SEM) of active material fracture surfaces

An effective method of determining the structure of the active material is to examine fracture surfaces in a scanning electron microscope. This can give valuable information on the composition and structural properties such as particle size, shape and porosity.

Samples were made by attaching a small piece of positive active material to a planchette with araldite adhesive. A thin layer of gold was applied using an Edwards sputter coater to improve conductivity and reduce charging. A coating time of 5 min was used. Samples were stored in a desiccator, until required for examination in the SEM, to prevent the adsorption of moisture and contamination.

All images were produced with secondary electrons using a JEOL 6310 scanning electron microscope. At high magnifications, the smallest spot size that could be used easily was selected. Working distances were reduced as much as possible to enhance image quality and a beam voltage of 15 kV was found to give good quality images.

4.4. BET surface area analysis

It is important to consider the surface area of the positive active material when studying batteries. It will have a direct influence on the way in which the battery operates since all electrochemical reactions that occur within a battery during operation, do so on the surface of the active materials.

Values of surface area are obtained by measuring the volume of gas required to form a monolayer on the sample surface (BET method). The gas used was nitrogen, which has a cross sectional area of 1.62×10^{-20} m^2.

The analysis was performed using a Micromeritics Gemini 2360 VS.OO. This equipment is used to measure the volume of gas adsorbed with change in pressure. BET surface area analysis was conducted on samples of positive active material after removal from the battery. Active material was removed from the battery grid and broken into pieces, small enough to fit into the sample tube. Care was taken not to break the pieces more than necessary, as this artificially increases the surface area and therefore the measured value.

4.5. X-ray diffraction (XRD)

XRD was used to determine the composition of the samples of positive active material from the cells examined. Standard data files from the Joint Committee for Powder Diffraction Standards (JCPDS) [2] were used to initially identify the phases present.

Quantitative analysis of a mixture can be obtained as the intensity of the peaks on a diffraction pattern, corresponding to a particular phase, are related to the proportion of that phase [3].

For the purposes of this study the computer program PEAKS, specifically designed for the quantitative analysis of materials, commonly found in the lead acid battery, was used [4]. The program is capable of determining the relative abundance of the lead phases commonly found at the different stages of lead acid battery manufacture and service. Peak intensities from the XRD patterns are entered into the ''input screen'' of the program and the relative abundance of each phase is calculated. Initial corrections are made for background radiation and peak overlap before average intensities are calculated for up to three of the peaks from each of the phases present. Data is then normalised for differences in scattering power using pre-determined calculated reference intensity ratios [5].

XRD samples were prepared from the dried plates by pushing a number of tablets from the centre of the grid and then grinding to a fine powder using a pestle and mortar. The ground powder was placed in an aluminium XRD holder with a glass slide back. This was then inserted into the X-ray diffractometer for analysis.

A Philips PW1730/00 diffractometer using Cu Kα radiation, was used for all analyses. Samples were scanned over a range of 5–90° in order to obtain background values at 9 and 19 for quantitative analysis using the PEAKS program. A scan speed of 0.5 s per step and a step size of 0.01° was used.

4.6. Interfacial analysis

The thickness and structure of the positive grid corrosion layer can provide important information as to why a battery cell has failed. An effective way to study these features is to examine a polished cross section using optical or electron microscopy.

Dried battery plates consist of a soft lead grid, having very low stiffness, surrounded by friable active material. When handling plates, great care must be taken to avoid unnecessary bending as this can lead to the formation of additional cracks in the active material and corrosion layer. To reduce the risk of damaging the plates after removal from the battery, they were initially encapsulated in resin in order to increase their durability. After encapsulation, the plates were cut and remounted into suitable sizes for polishing.

Several polishing stages were used to prepare the samples. Initially, they were flattened using 300–1200 grit size silicon carbide paper with a platen speed of 150 rpm. Water was used as a lubricant and only light pressure was applied to the sample. Texmet polishing cloth loaded with five and then 0.3 μm alumina suspension was used for the second stage. Finally, a texmet cloth with masterpolish was used on a Buehler Vibromet vibratory polisher, for approximately 30 min.

4.7. Measurement of corrosion layer thickness

An optical microscope with camera attachment was used to record images of grid wires showing the corrosion layer. The thickness of the corrosion layer was measured at various positions on the grid wire using Optimas 6 image analysis software [6].

4.8. Electron probe microanalysis

A Jeol JXA-8600 superprobe was used to determine the composition of the corrosion layer on the good cell of the battery cycled 92 times, as this was of a reasonable thickness and a typically representative structure of the layer observed on the other batteries. Readings were taken in a line across the corrosion layer at 1 μm intervals. An initial qualitative analysis indicated that the corrosion layer consisted of lead, oxygen and sulphur. Results were used to calculate the oxygen to lead ratio for each analysis. To prevent charging effects, the samples were coated with a thin layer of carbon, using an Edwards sputter coating unit. Samples and standards were coated simultaneously to reduce errors caused by adsorption of X-rays by the coating layer.

5. Results and discussion

5.1. Cycling of batteries

The batteries examined in this study were all cycled until their capacity reached a value of 80% of the starting capacity. The number of cycles required for this state to be reached varied between individual batteries. The results presented are based on eight batteries from the same batch,

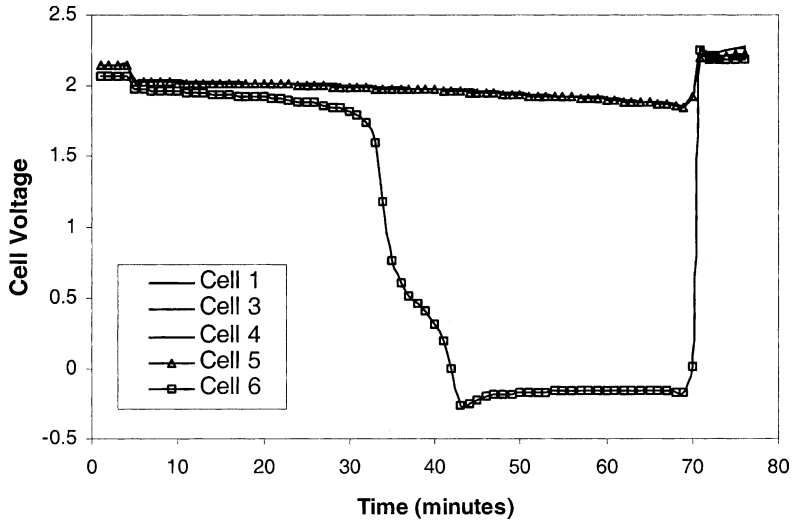

Fig. 4. Plot of potential vs. time for cells in battery cycled 10 times.

which failed after 10, 28, 42, 49, 65, 73, 92 and 133 cycles. An additional battery from this batch was examined in the freshly formed state for comparison with the cycled batteries.

5.2. Electrical testing of batteries

When a battery is cycled, its capacity will gradually reduce to a lower value at the end of each discharge/charge cycle. This is caused by degradation of the electrodes within the battery. The test batteries consisted of a 12 V monobloc containing six cells, each producing just over 2 V. The reduction of the capacity of a battery during charging is caused by a reduction in capacity of the individual cells. However, the degree to which the capacity has reduced in each cell generally varies. The capacity of a cell is directly related to its drop in voltage during discharge. Figs. 4–11 show plots of cell voltage versus time for a final discharge/charge cycle after the battery had reached its failure point.

In Figs. 4–11, the variation in potential of the good cells is plotted with triangles, the bad cells with squares, and the intermediate cells with a plane line. The plots demonstrate that the cells within each battery have degraded by varying amounts. In some instances, there is a clear example of a failed cell, with a very low potential, compared to the other cells in the battery which all have high potentials. In other batteries, all the cells appear to fail to a certain extent and there is no clearly defined good or bad cell. Fig. 4 shows a typical example of a battery with a single bad cell where all the other cells are good, in comparison Fig. 8 is from a battery where all the cells have, to a certain extent failed. Previous research on batteries with similar plates [7] indicated that the positive, as opposed to the negative plates, were the capacity limiting factor.

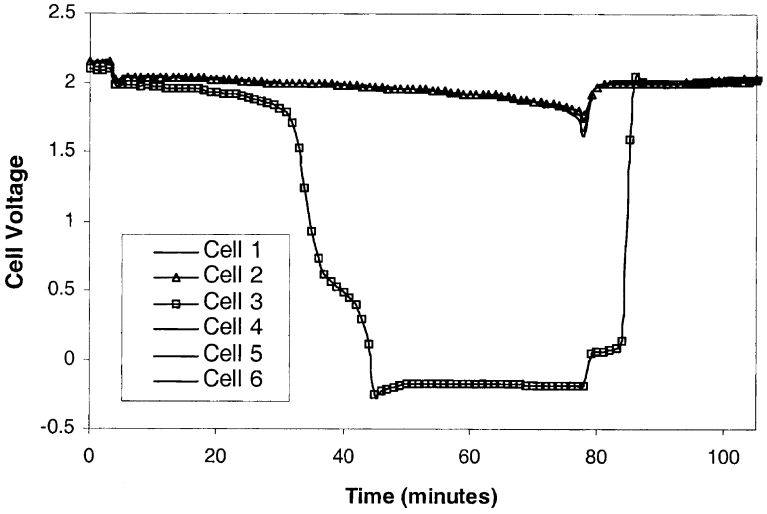

Fig. 5. Plot of potential vs. time for cells in battery cycled 28 times.

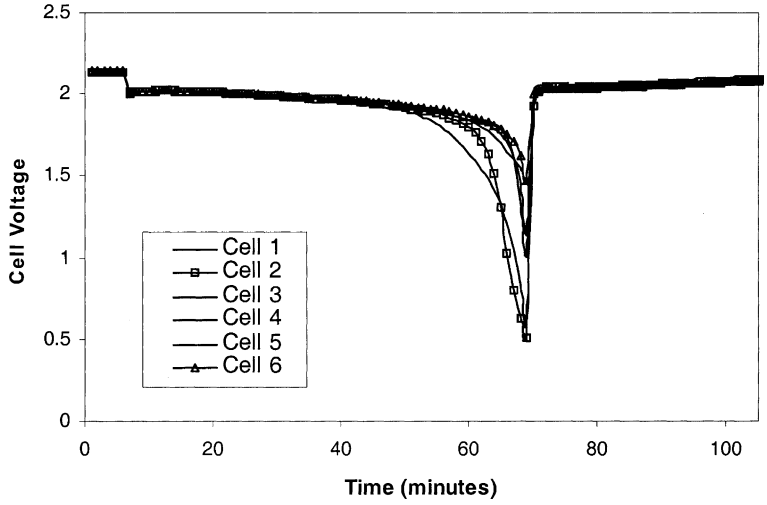

Fig. 6. Plot of potential vs. time for cells in battery cycled 42 times.

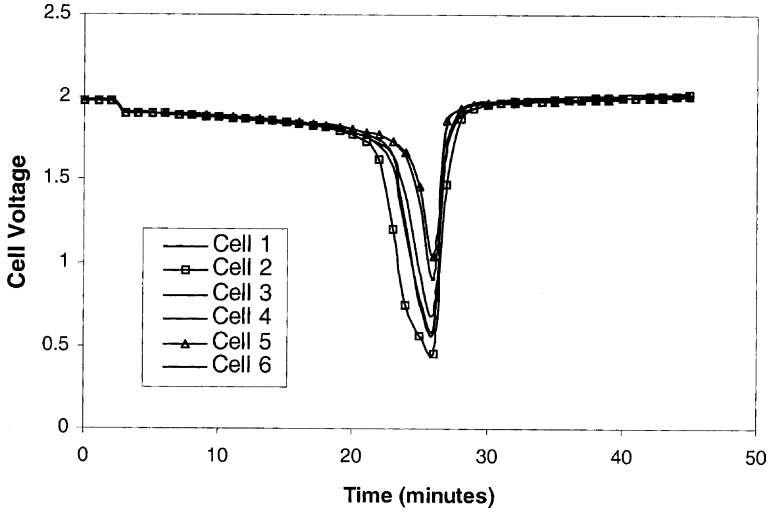

Fig. 7. Plot of potential vs. time for cells in battery cycled 49 times.

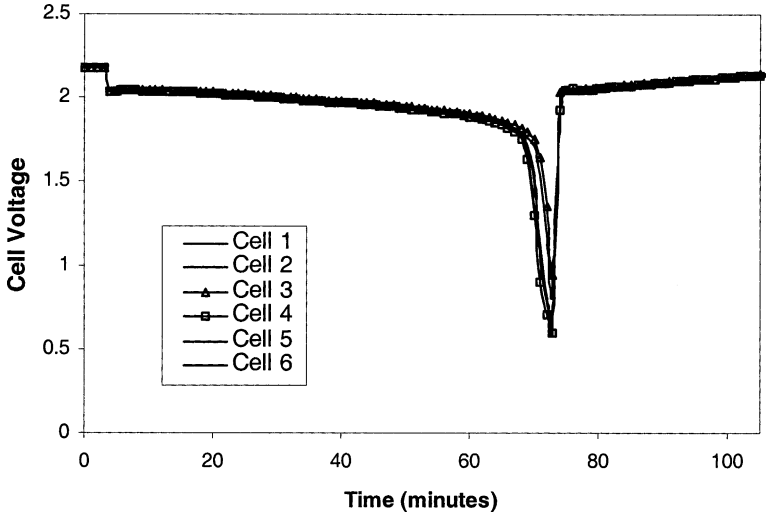

Fig. 8. Plot of potential vs. time for cells in battery cycled 65 times.

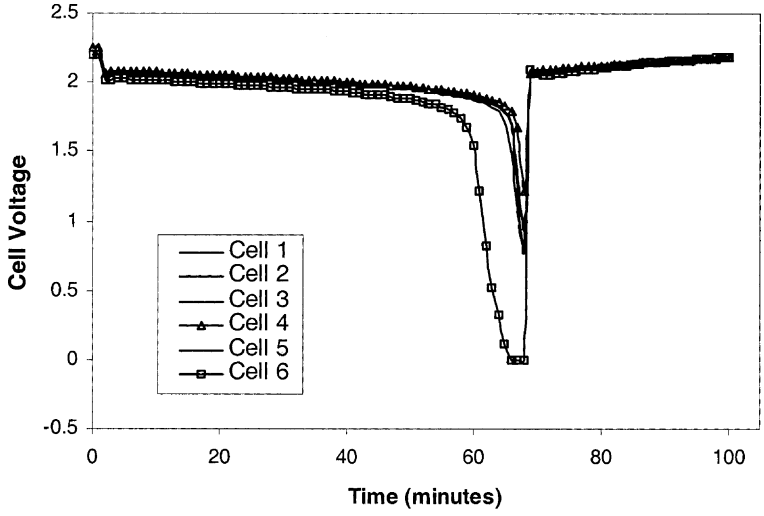

Fig. 9. Plot of potential vs. time for cells in battery cycled 73 times.

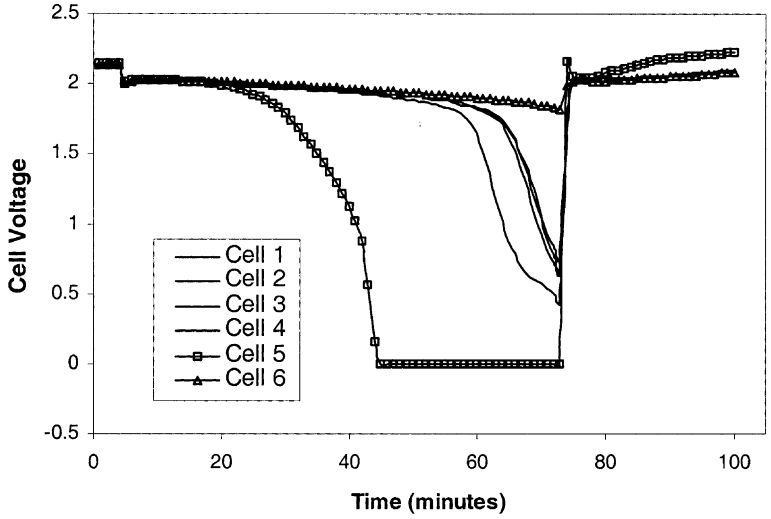

Fig. 10. Plot of potential vs. time for cells in battery cycled 92 times.

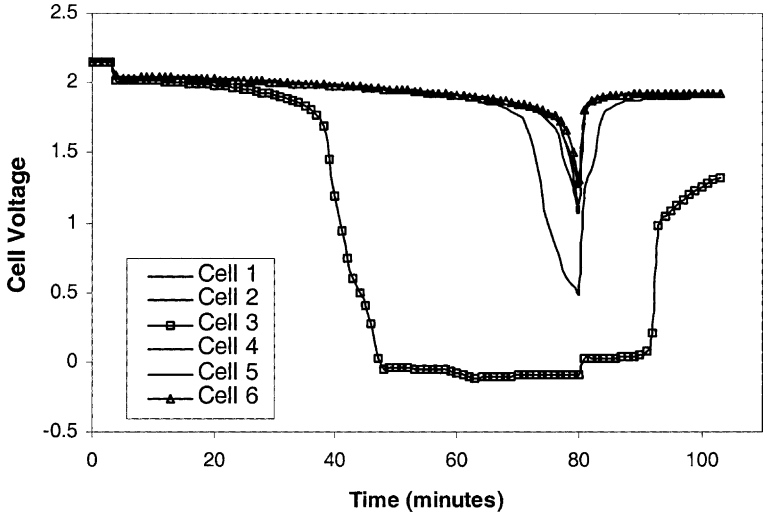

Fig. 11. Plot of potential vs. time for cells in battery cycled 133 times.

Table 1
Specific gravity of electrolyte at top and bottom of separators in good and bad cells of cycled batteries

Number of cycles	Good cell ($\times 10^3$)			Bad cell ($\times 10^3$)		
	SG top	SG bottom	ΔSG (bottom–top)	SG top	SG bottom	ΔSG (bottom–top)
0	1315	1315	0	–	–	–
10	1325	1330	5	1275	1280	5
28	1330	1345	15	1295	1305	10
42	1330	1345	15	1330	1360	30
49	1310	1330	20	1315	1330	15
65	1310	1335	25	1285	1325	40
73	1315	1360	45	1285	1340	55
92	1315	1320	5	1315	1330	15
133	1345	1350	5	1330	1360	30

5.3. Electrolyte SG

Acid stratification occurs when the acid concentration varies at different positions on the separator paper. Sulphuric acid concentration in the electrolyte is directly related to the SG, which can be determined easily with a small sample of acid. For each of the cells examined, the SG was measured at the top and bottom of the separator. Values obtained are shown in Table 1. The greater the difference between these two values the larger the amount of stratification.

Acid stratification as a function of number of cycles is shown in Fig. 12. The top of each bar represents the SG at the bottom of the cell and the bottom of each bar, the SG at the top. Bar length therefore gives the degree of stratification. There is a general trend demonstrating greater stratification in the bad cell compared to the good. The only exception to this is in the batteries cycled 28 and 49 times.

The batteries cycled between 0 and 73 times show an increase in stratification with number of cycles. This trend is not reflected in the results obtained from the batteries cycled 92 and 133 times. There is no obvious explanation for this trend.

It should also be noted that the majority of cells have electrolyte specific gravities greater than that of the freshly formed battery. This increase in sulphuric acid concentration suggests water loss, which may contribute to a decrease in battery capacity.

5.4. Positive active material

5.4.1. Compositional analysis

During battery cycling, a number of compositional and structural changes occur within the positive active material. This is most apparent with reference to the compositional

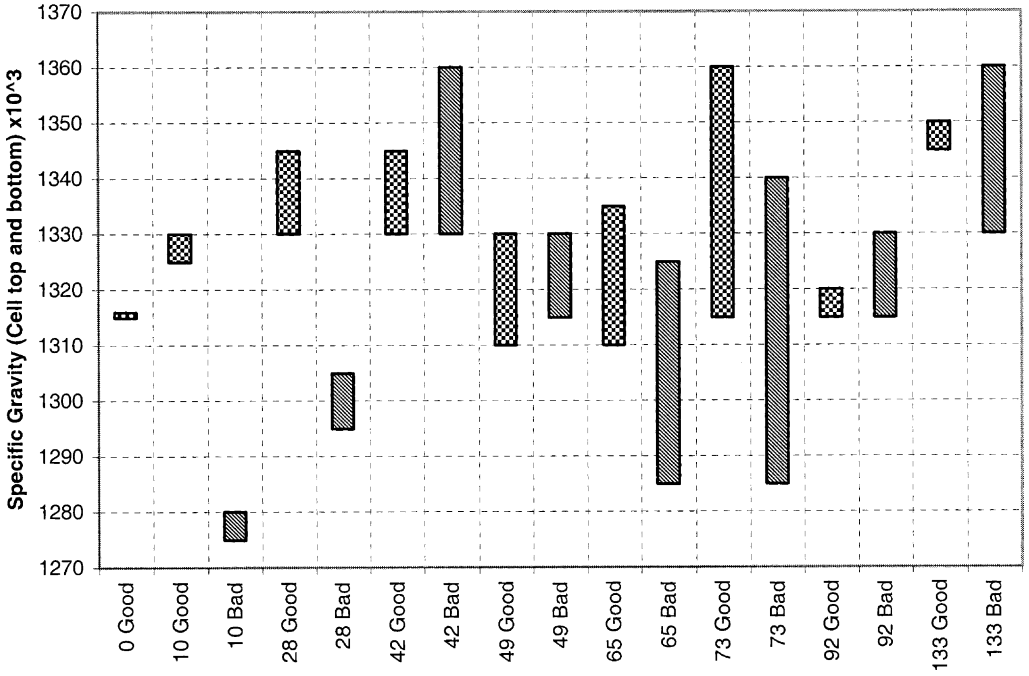

Fig. 12. Difference in specific gravity between top and bottom of separator papers in good and bad cells.

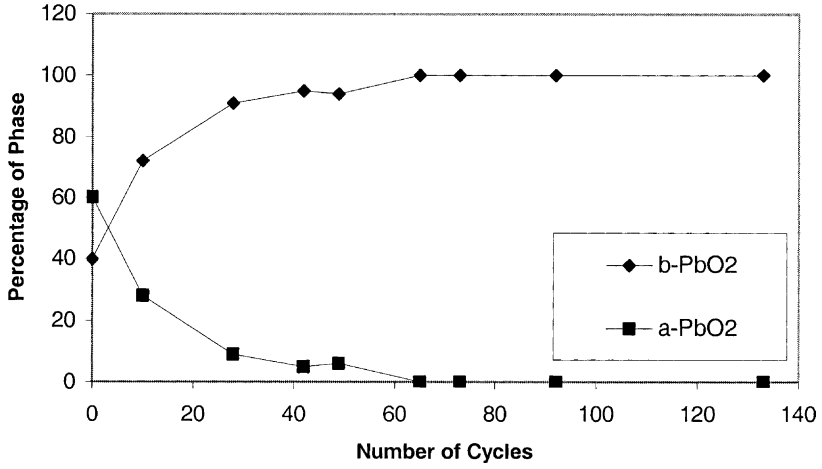

Fig. 13. Composition of positive active material from good battery cells.

analysis obtained from the X-ray diffraction patterns. Fig. 13 shows the composition of the positive active material from the good cells of the cycled batteries.

The active material consists of a mixture of alpha-lead dioxide (α-PbO_2, orthorhombic), and beta-lead dioxide (β-PbO_2, tetragonal). As the battery is cycled, the proportion of the alpha phase decreases. This phenomenon is well documented, [8] and occurs because the alpha phase cannot be formed in acidic environments. The rate at which the alpha lead dioxide is converted to beta lead dioxide reduces with number of cycles due to the diminishing fraction of alpha phase.

The composition of the positive active material in the bad cells is shown in Fig. 14. Increase in beta lead dioxide with number of cycles similar to that observed in the good cells is shown in Fig. 14. However, the batteries cycled 10 and 28 times contain large amounts of lead sulphate. Lead sulphate is formed during discharge of the battery and is consequently converted back into lead dioxide on charging. This has not occurred in these cells and the remnant lead sulphate is present. Examination using the scanning electron microscope identified large lead sulphate crystals in the battery cycled 28 times. These varied in size from a few microns to greater than 10 microns, see Figs. 15 and 16.

From a kinetic standpoint, once sulphate crystals of this size are formed, it is unfavourable for them to react to form lead dioxide and sulphuric acid due to their high volume and low surface area. Given the amount of lead sulphate present, it is not surprising that these cells have failed and it is almost certain that sulphation was the cause of capacity loss and eventual battery failure. This is reflected by the very low SG measured in these cells, which suggest incomplete charging.

When a comparison is made between the quantities of alpha and beta lead dioxide in the good and bad cells of the batteries cycled 10 and 28 times, the proportion of alpha lead dioxide is reduced whereas the proportion of the beta phase is similar. This suggests that the lead sulphate in these batteries had formed mainly from alpha lead dioxide as opposed to beta lead dioxide.

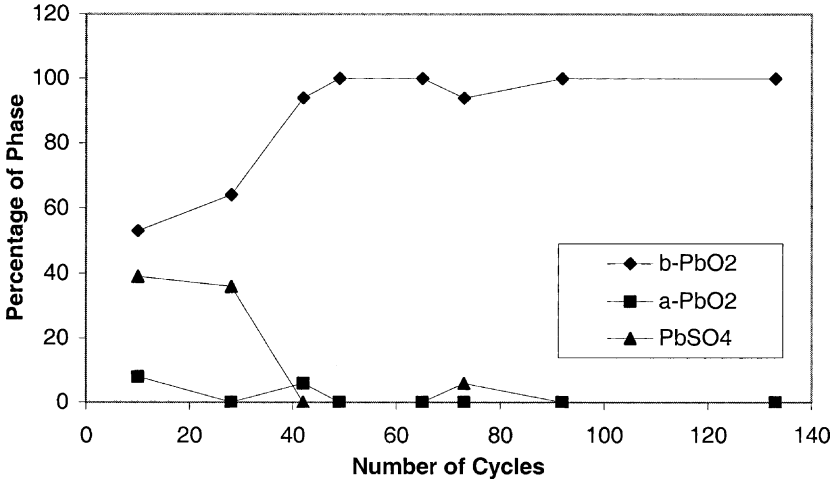

Fig. 14. Composition of positive active material from bad battery cells.

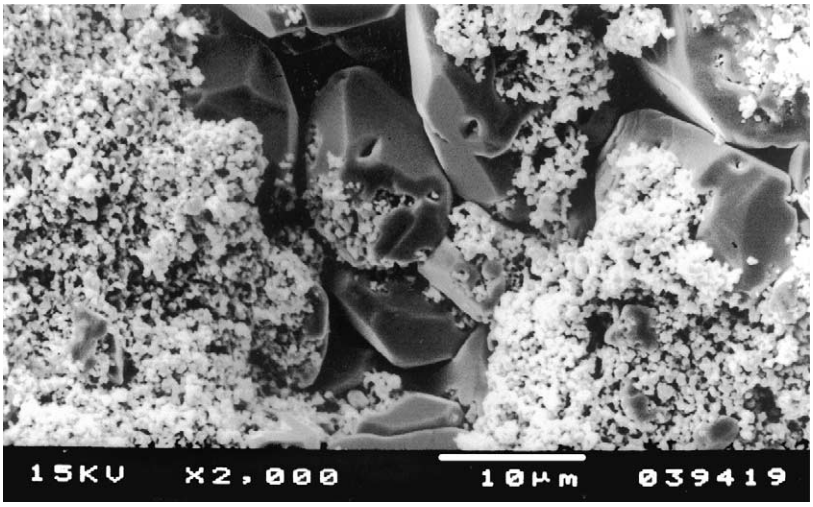

Fig. 15. Sulphate crystals in bad cell of battery cycled 28 times (2000×).

5.4.2. Surface area analysis

Variations in BET surface area with number of cycles are shown in Fig. 17. BET surface area for the good cell in every battery is consistently higher than that in the corresponding bad cell, as shown in Fig. 17. However, there does not appear to be any consistent trend between BET surface area and number of cycles. The positive active material in the freshly formed battery has a surface area around 3.5, which then drops to a value comparable with that of the bad cell after approximately 40 cycles. This reduction in surface area with cycles is not observed in the bad cells (batteries cycled 10 and 28 times). Lead sulphate has a low surface area compared to lead dioxide and its presence is the most likely cause of the low measured surface areas of the plates in these batteries.

5.5. Corrosion layer thickness measurements

During operation and overcharging of a battery, oxygen gas reacts with the positive grid forming a lead monoxide corrosion layer. This subsequently reacts electrochemically to form lead dioxide resulting in the formation of a corrosion layer containing both, lead monoxide and lead dioxide. Corrosion layer thickness measurements were taken on the top, bottom, left and right hand sides of the grid wire in the good and bad cells of cycled batteries. The average corrosion layer thickness versus the number of cycles for good and bad cells is shown in Fig. 18.

With the exception of the corrosion layer thickness measured on the battery cycled 49 times, which was significantly thicker than that on the other grids, the data appears to follow an exponential relationship. Equations of the curves in Fig. 18, assuming an exponential relationship, are shown with corresponding "best fit" R^2 values.

- Good cells $y = 16.4\,e^{0.0106x}$ $R^2 = 0.987$
- Bad cells $y = 8.3\,e^{0.0247x}$ $R^2 = 0.996$

From the figure and equations, it can be seen that the rate of corrosion layer thickening increases with number of cycles and is greatest in the bad cells. This observation

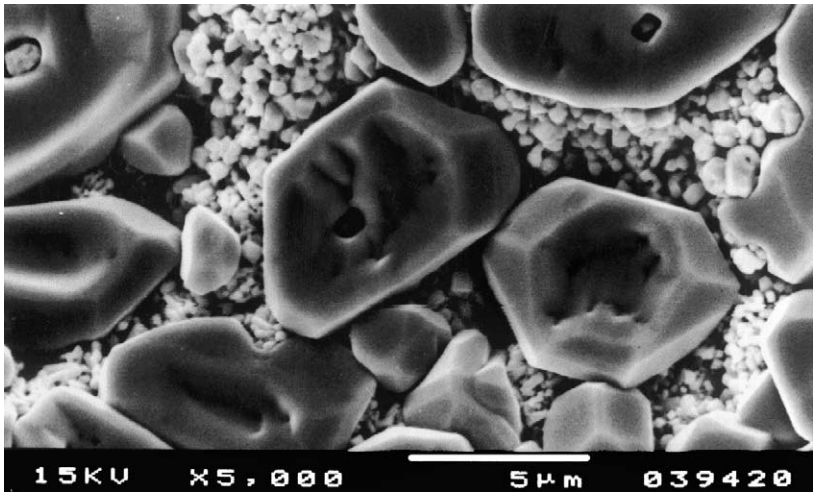

Fig. 16. Sulphate crystals in bad cell of battery cycled 28 times (5000×).

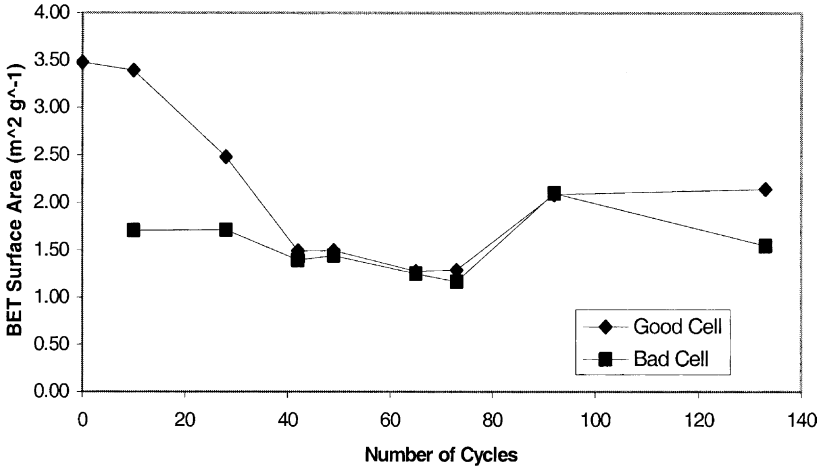

Fig. 17. BET surface area of positive active material in cycled batteries.

can be explained by considering the processes that occur during cycling of the battery. Corrosion layer growth occurs during overcharging when oxygen evolved within the positive active material diffuses to the positive grid and reacts to form lead oxide. This is shown by Eqs. (1)–(3).

$$2Pb + O_2 \rightarrow 2PbO \quad (1)$$

$$PbO + (n-1)O \rightarrow PbO_n (1 < n < 2) \quad (2)$$

$$PbO_n + (2-n)O \rightarrow PbO_2 \quad (3)$$

It follows that corrosion layer growth rate and therefore its thickness is related to overcharging time. The amount of overcharging, that a battery cell sustains, is a function of the charging time (16 h for these batteries) and the capacity or length of time needed to charge the cell. A consequence of battery cycling is a reduction in the capacity of the cells. It follows therefore that a reduced capacity cell, for example the bad cell, may charge more rapidly than the good cell in the same battery, effectively increasing the overcharging time. The increased corrosion layer thickening observed in the bad cells compared to the good cells could therefore be accounted for by the reduced capacity of the bad cells. The process of thickening of the corrosion layer is thus one of cumulative damage. It should be noted however, that the recharge potential of 14 V, although relatively high, was the standard potential used throughout the experiments. It is recognised that recharging at a lower potential for a longer period could reduce the rate of positive corrosion layer thickening, possibly extending the cycle life of the battery.

It is apparent from the results that the battery cycled 49 times behaved in a different manner as compared to all other batteries tested. Additionally, the corrosion layer thickness in both the good and bad cells of this battery were unusually thick. It is therefore not unreasonable to suggest that a different failure mechanism or combination of failure mechanisms has been operative in this battery. Further work would be required to understand the actual mechanisms of failure.

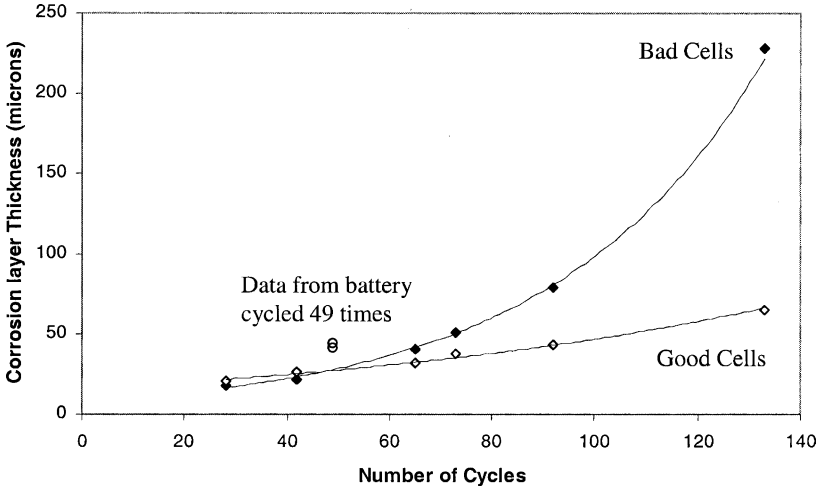

Fig. 18. Corrosion layer thickness vs. number of cycles for good cells.

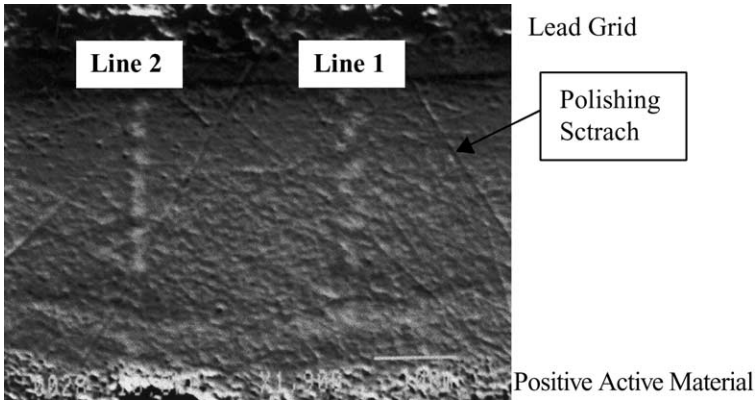

Fig. 19. Secondary electron image showing area of corrosion layer analysed using EPMA.

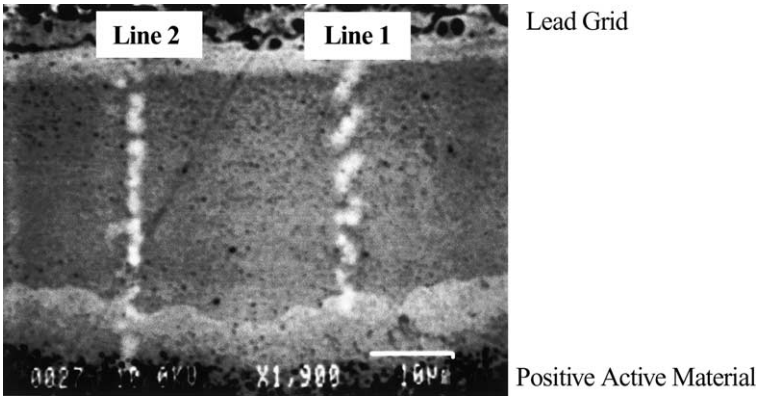

Fig. 20. Backscattered electron image showing area of corrosion layer analysed using EPMA.

5.6. Electron probe microanalysis

Quantitative analysis of the positive grid corrosion layer using electron probe microanalysis revealed a variation in the concentration of oxygen with distance across the corrosion layer section. Secondary and backscattered electron images of the position of each trace where the concentration of oxygen was measured is shown in Figs. 19 and 20. The thickness of the corrosion layer is approximately 40 μm.

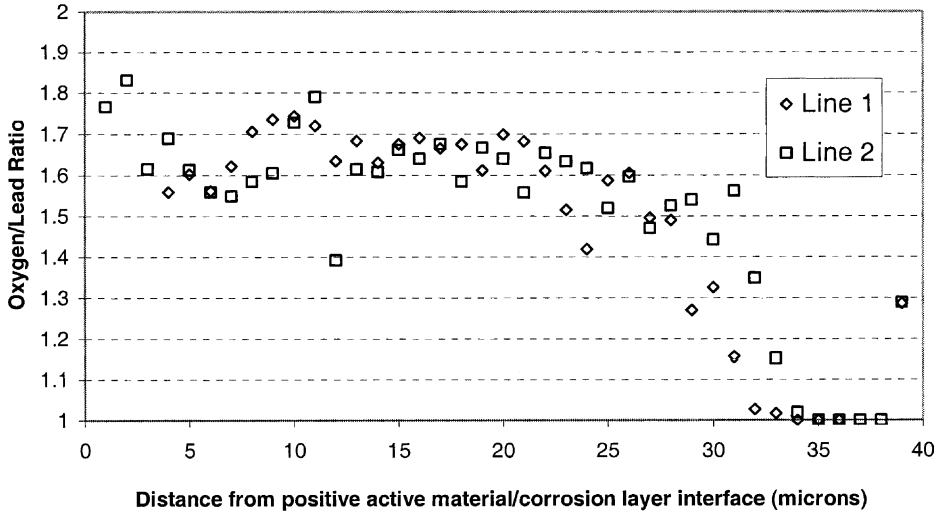

Fig. 21. Compositional analysis of corrosion layer from battery used to study cycling performance.

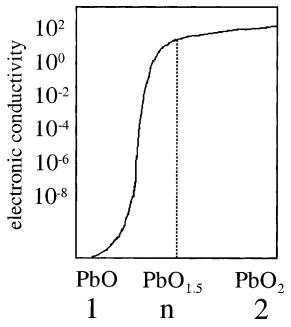

Fig. 22. Variation in electronic conductivity of lead oxide with oxygen concentration [7].

From Fig. 19, it is apparent that the corrosion layer section has a reasonably flat surface. This is important as the accuracy of electron probe microanalysis is sensitive to surface roughness. The backscattered image, Fig. 20, does not indicate the presence of any porosity, which can contribute to errors in the compositional analysis.

The variation in oxygen/lead ratio for two line scans across the corrosion layer section is shown in Fig. 21. A consequence of the variation in concentration of oxygen, or stoichiometry of the oxide, is a change in conductivity. It has been shown that the conductivity of the oxide decreases dramatically with oxygen concentration, this is shown diagrammatically in Fig. 22 [9].

Oxygen to lead ratio greater than 1.5, for the majority of the corrosion layer thickness as shown in Fig. 21, suggests high conductivity. However, this value drops to between 1 and 1.5 for a band of the corrosion layer approximately 10 μm in thickness adjacent to the lead grid. It is suggested that the reduction in oxygen concentration is caused because the oxygen must diffuse through the outer regions of the corrosion layer before reaching this position. Low oxygen concentrations are consistent with the formation of a thin passivating layer of lead monoxide adjacent to the corrosion layer which has been reported in previous literature [10]. The presence of lead monoxide is normally associated with the reaction of lead dioxide with lead during self discharge, according to Eq. (4).

$$PbO_2 + Pb \rightarrow 2PbO \quad (4)$$

6. General discussion

A number of possible causes for failure have been identified. For the batteries, which sustained the least numbers of cycles, 10 and 28, the most likely cause of failure is sulphation of the positive electrode, Figs. 14–16. The sulphation was restricted to the bad cells of the battery, which showed a rapid reduction in voltage, and therefore capacity, Figs. 4 and 5, during the final discharge/charge cycle compared to the remaining five cells which all showed similar performance.

Failure of the batteries that sustained a high number of cycles, 92 and 133, is considered to be due to the large corrosion layer thickness observed on the bad cells, Fig. 18. The plots of cell voltage versus time, Figs. 10 and 11 indicate that these cells showed a reduction in voltage much earlier than the remaining cells.

The batteries that failed at an intermediate number of cycles, 42, 49, 65 and 73, did not have component cells which exhibited significantly different behaviour, Figs. 6–9. This suggests that all the cells failed gradually, at the same rate, during cycling. Failure was due to a continuous degradation of the active materials rather than as a consequence of a particular failure mechanism affecting one specific aspect of battery performance. BET surface areas, Fig. 17, are similar for both good and bad cells, which is consistent with this observation. This type of failure is commonly referred to as premature capacity loss [11].

7. Conclusions

The following conclusions can be drawn from the results and discussion:

1. When a battery fails, the cells within the battery degrade to different levels.
2. Sulphation of the positive plates is the most likely cause of failure in the batteries cycled 10 and 28 times. This suggests that if the cells have not failed due to sulphation, within the first 30 cycles, sulphation is unlikely to be the cause of subsequent failures.
3. Lead sulphate forms more readily at the expense of α-lead dioxide rather than β-lead dioxide.
4. Resistivity of the negative active material does not vary significantly during battery cycling.
5. Acid stratification is greater in the bad cells of a battery that indicates a lower capacity.
6. The corrosion layer thickness is greater in the bad cells.
7. Corrosion layer growth rate is greater in the bad cells.
8. The battery formed a passivating lead monoxide corrosion layer adjacent to the positive grid.

References

[1] W. Mindt, Electrical properties of electrodeposited PbO_2 films, J. Electrochem. Soc. 116 (8) (1969) 1076–1080.
[2] Joint committee for powder diffraction standards, PDF-2 Database Sets 1–45, International Centre for Diffraction Data, 12 Campus Boulevard, Newtown Square, PA, USA, 1995, pp. 19073–3273.
[3] R. Jenkins, J.L de Vries, An introduction to X-ray powder diffraction, in: N.V. Philips (Ed.), Gloeilampenfabrieken, Eindhoven, Holland, The Netherlands.
[4] D.A.J. Rand, R.J. Hill, M. McDonagh, Improving the curing of positive plates for lead/acid batteries, J. Power Sources 31 (1990) 203–225.
[5] K. Harris, R.J. Hill, D.A.J. Rand, Crystalline phase composition of positive plates in lead/acid traction batteries under simulated electric vehicle service, J. Power Sources 8 (1982) 175–196.
[6] OPTIMAS 6.1, Optimas UK Ltd., West Maling, Kent, UK.

[7] R.J. Ball, R. Kurian, R. Evans, R. Stevens, Study of valve regulated lead/acid batteries manufactured with different separator papers, J. Power Sources 104 (2) (2002) 234–240.
[8] D. Berndt, Maintenance-Free Batteries, A handbook for battery technology, 2nd Edition, Wiley, p. 314.
[9] F. Lappe, Some physical properties of sputtered PbO_2 films, J. Phys. Chem. Solids 23 (1962) 1563–1572.
[10] D. Pavlov, A theory of the grid/positive active-mass (PAM) interface and possible methods to improve PAM utilization and cycle life of lead/acid batteries, J. Power Sources 53 (1995) 9–21.
[11] K.K. Constanti, A.F. Hollenkamp, M.J. Koop, K. McGregor, Physical change in positive-plate material—an underrated contributor to premature capacity loss, J. Power Sources 55 (1995) 269–275.